

## **Probing the Electronic Relaxation Pathways and Photostability of the Synthetic Nucleobase Z via Laser Interfaced Mass Spectrometry**

William Whitaker, Katya E. Moncrieff, Cate S. Anstöter, Natalie G. K. Wong, Jacob A. Berenbeim and Caroline E. H. Dessent\*

Department of Chemistry, University of York, Heslington, YO10 5DD, U. K.

\* E-mail: [caroline.dessent@york.ac.uk](mailto:caroline.dessent@york.ac.uk)

### **Supporting Information**

S1: Laser Power Dependency of Photodepletion Experiments.

S2: Calculated Relative Zero-Point Energies for Protomers of Z Using Various Functionals and Basis sets.

S3: Comparison of Calculated TDDFT Electronic Absorption Spectra Using Various Functionals and Basis sets.

S4: Excited states of the protonated Z isomers

S5: Complete Table of Fragments Observed on UV Laser Excitation and During HCD Experiments.

S6: Photofragment Production Spectra for Minor Photofragments.

S7: High-Energy Collision-Induced Dissociation Spectra.

S8: Histograms Showing the Relative Ion Yields of Photofragments and HCD Fragments.

S9: Cartesian coordinates of the Protomers of Z

### S1: Laser Power Dependency of Photodepletion Experiments.

To verify that a single-photon absorption process is occurring for photofragmentation experiments, a power study was performed for protonated Z ions near the band I absorption maximum (320 nm, 3.87 eV) under experimental parameters (ion accumulation time: 100 ms; fragmentation time: 100 ms). A linear relationship between photodepletion and laser power with a large  $R^2$  value is representative of single photon absorption dependence across the working range.

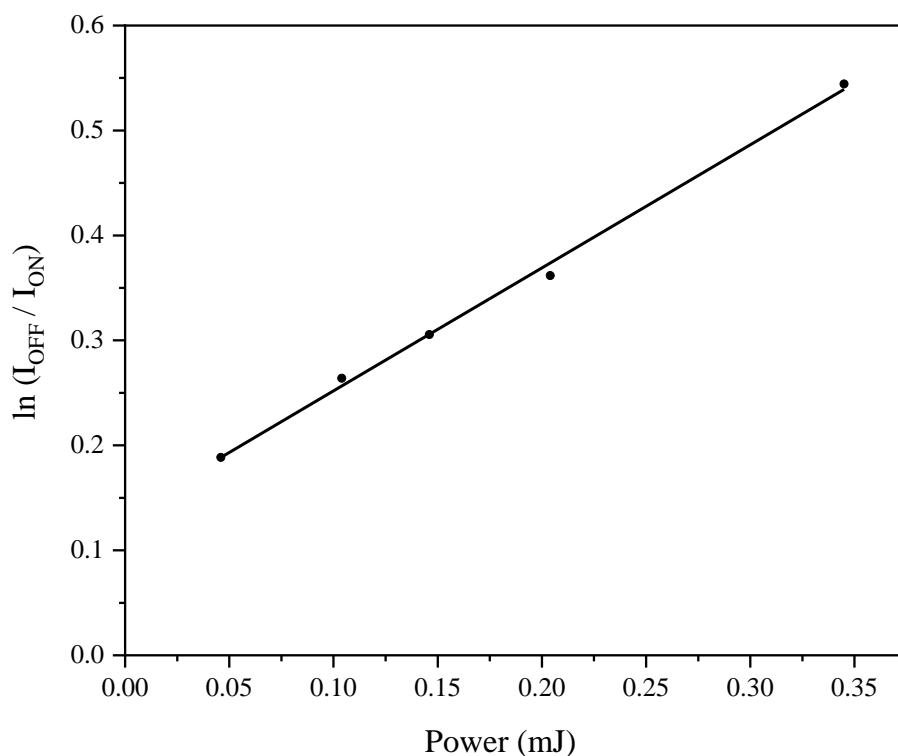


**Figure S1:** Power study for  $[Z+H]^+$  ions produced via electrospray ionisation from a solution of water. Measurements acquired over the experimental working range for laser power (0.045-0.345 mJ) near the band I absorption maximum (320 nm, 3.87 eV). Dots show individual data points and the line represents the linear regression of the data ( $R^2 > 0.99$ ).

## S2: Calculated Relative Zero-Point Energies for Protomers of Z Using Various DFT Functionals.

The lowest energy structures for protomers of Z were identified by optimising the structures for a variety of potential protomers and calculating the relative zero-point energies (ZPEs) of each. Calculated energies of each of the lowest energy protomers using three DFT functionals, and both the Pople and Dunning basis sets, are shown in Table S1.

**Table S1:** Calculated relative energies for protomers of Z using various DFT functionals and basis sets. All energies have been zero-point energy corrected.

	Relative energy / eV			
	PBE0/6-31+G**	M06-2X/6-31+G**	$\omega$ B97XD/6-31+G**	$\omega$ B97XD/cc-pVTZ
<b>enol-N4</b>	0.00	0.00	0.00	0.00
<b>enol-N7O</b>	0.14	0.11	0.19	0.21
<b>keto-N7O</b>	0.26	0.26	0.28	0.29

As noted in the main text (section 3.1), protonation at nitrogen within the heterocycle will yield the most stable gaseous cation of Z. Table S1 indicates that this result is consistent across all functionals and basis sets used which supports the conclusion that the enol-N4 protomer will be the most stable (hence will have the greatest population in a mixture of isomers). Furthermore, despite some discrepancy in the energy difference between enol-N4 and enol-N7O depending on the functional used, the magnitude of the energy difference is consistently sufficient to suggest that the proportion of  $[Z+H]^+$  existing as enol-N7O in a sample compared to enol-N4 will be low. Keto-N7O is also always calculated to be the least stable protomer shown with a relative energy of greater than +0.26 eV regardless of functional or basis set.

### S3: Excited states of the protonated Z isomers

Vertical excitation energies, raw and shifted, for the bright singlet  $\pi\pi^*$  transitions in the experimentally relevant range, calculated using TDDFT at different levels of theory. The results are shown for all three of the lowest energy protomers of Z. The experimental results are also given for ease of comparison.

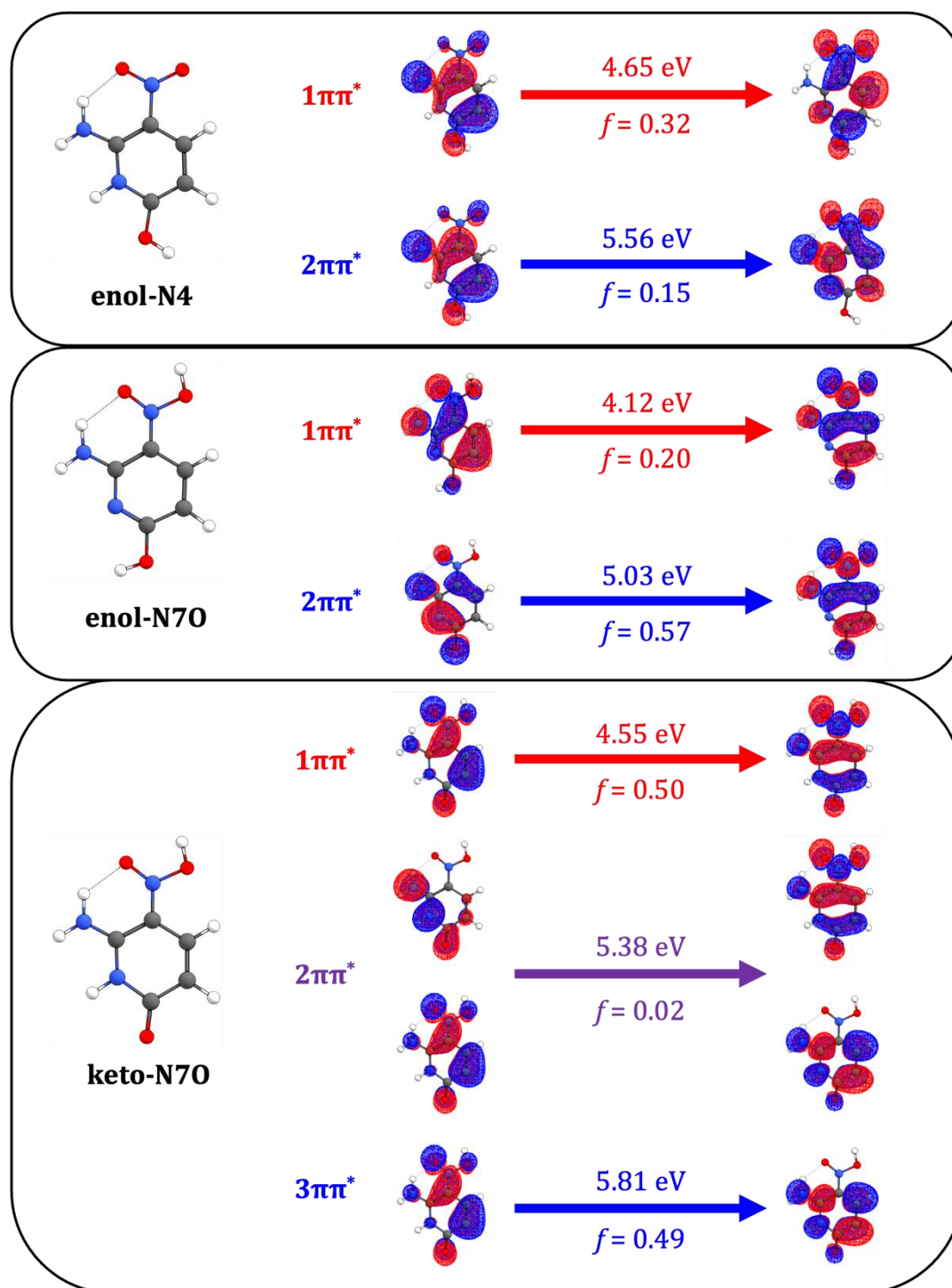
enol-N4	VEE / eV		Shifted VEE / eV		$\Delta E$ / eV
	1 $\pi\pi^*$	2 $\pi\pi^*$	1 $\pi\pi^*$	2 $\pi\pi^*$	
PBE0/6-31+G**	4.656	5.582	4.156	5.082	0.926
M06-2X/6-31+G**	4.219	5.109	3.719	4.609	0.890
$\omega$ B97XD/6-31+G**	4.638	5.561	4.138	5.061	0.923
$\omega$ B97XD/cc-pVTZ	4.448	5.377	3.948	4.877	0.928

enol-N70	VEE / eV		Shifted VEE / eV		$\Delta E$ / eV
	1 $\pi\pi^*$	2 $\pi\pi^*$	1 $\pi\pi^*$	2 $\pi\pi^*$	
PBE0/6-31+G**	4.120	5.028	3.620	4.528	0.908
M06-2X/6-31+G**	3.538	4.413	3.038	3.913	0.876
$\omega$ B97XD/6-31+G**	4.104	5.017	3.604	4.517	0.912
$\omega$ B97XD/cc-pVTZ	3.798	4.755	3.298	4.255	0.957

keto_N70	VEE / eV		Shifted VEE / eV		$\Delta E$ / eV
	1 $\pi\pi^*$	2 $\pi\pi^*$	1 $\pi\pi^*$	2 $\pi\pi^*$	
PBE0/6-31+G**	4.531	5.874	4.031	5.374	1.343
M06-2X/6-31+G**	3.877	5.252	3.377	4.752	1.376
$\omega$ B97XD/6-31+G**	4.514	5.869	4.014	5.369	1.355
$\omega$ B97XD/cc-pVTZ	4.139	5.616	3.639	5.116	1.478

Experiment	Band I / eV	Band II / eV	$\Delta E$ / eV
MeCN-ESI	3.8	4.8	1.0
H <sub>2</sub> O-ESI	3.9	4.9	1.0

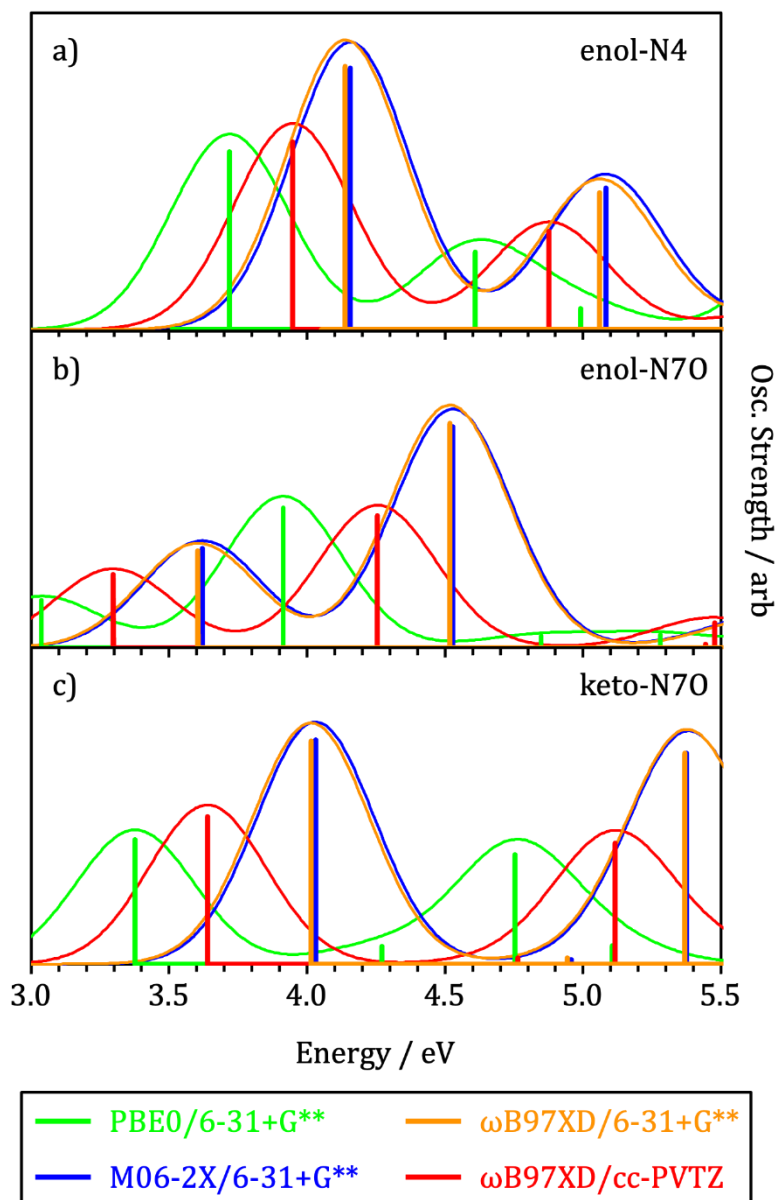
Schematic representation of the bright singlet  $\pi\pi^*$  states of the three protomers of Z, calculated using TDDFT at the  $\omega$ B97XD/cc-pVTZ level of theory. The molecular orbitals involved in the electronic states are shown, alongside the vertical excitation energy and the oscillator strength. N.B the keto-N7O has a  $2\pi\pi^*$  state with negligible oscillator strength that is not pictured.



**Figure S2:** A schematic showing the transitions involved in the low lying singlet  $\pi\pi^*$  excited states, with the red-shifted VEEs, oscillator strengths and relevant molecular orbitals for each protomer.

#### S4: Comparison of Calculated TDDFT Electronic Absorption Spectra Using Various DFT Functionals.

Shown in Figure S3 are TDDFT spectra for the low energy protomers of Z calculated at the PBE0/6-31+G\*\* (blue), M06-2X/6-31+G\*\* (green),  $\omega$ B97XD/6-31+G\*\* (orange) and  $\omega$ B97XD/cc-pVTZ (red) levels of theory. The purpose of this comparative study was to determine the effect of changing DFT functional on calculations of this system and to determine which functional was selected for calculations throughout the report.



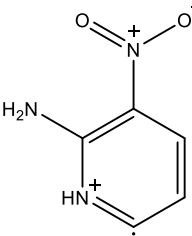
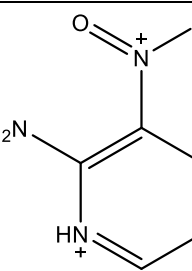
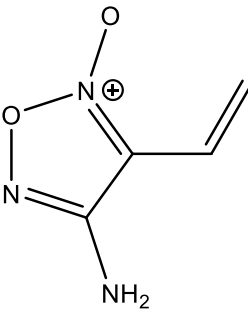
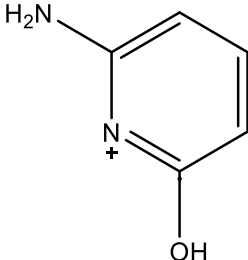
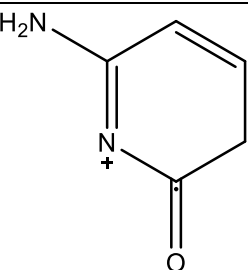
**Figure S3:** Comparison of calculated TDDFT excitation energies for enol-N4, enol-N7O and keto-N7O protomers of Z using a variety of DFT functionals. Oscillator strengths (Osc.) of individual transitions are given by the vertical bars, while the full line spectra are a convolution of the calculated spectrum with a Gaussian function (0.25 eV FWHM).

Figure S3 highlights the need for careful consideration of the choice of both functional and basis set when calculating the UV-Vis spectra of gas phase cations.

Interestingly, pronounced differences can be seen for the  $\omega$ B97XD functional when changing the basis set. The cc-pVTZ Dunning basis set is considerable larger than the 6-31+G\*\* basis set, resulting in a more balanced description of the electronic structure of the Z-protomers. For this reason, the  $\omega$ B97XD/cc-pVTZ level of theory was chosen to model the physical properties.

### S5: Complete Table of Fragments Observed from Photo- and Thermal Decay Pathways

**Table S2:** Proposed assignments of cationic photofragments and associated neutral fragments of  $[Z+H]^+$  ( $m/z$  156) observed following photoirradiation and thermalisation.

$m/z$	Formula	Tentative structure	H <sub>2</sub> O-ESI HCD (int.)	MeCN-ESI HCD (int.)	Photofragment H <sub>2</sub> O-ESI (int.)
156.040	C <sub>5</sub> H <sub>6</sub> N <sub>3</sub> O <sub>3</sub>	Z·H <sup>+</sup>			
139.038	C <sub>5</sub> H <sub>5</sub> N <sub>3</sub> O <sub>2</sub>		✓ (m)	✓ (m)	✓ (s)
138.030	C <sub>5</sub> H <sub>4</sub> N <sub>3</sub> O <sub>2</sub>		✓ (w)	✓ (w)	×
127.050	C <sub>4</sub> H <sub>5</sub> N <sub>3</sub> O <sub>2</sub>		✓ (vw)	×	×
110.036	C <sub>5</sub> H <sub>6</sub> N <sub>2</sub> O		✓ (vw)	✓ (vw)	✓ (m)
109.040	C <sub>5</sub> H <sub>5</sub> N <sub>2</sub> O		✓ (vw)	✓ (vw)	✓ (w)



99.056	$C_3H_5N_3O$		✓ (vw)	×	×
96.008	$C_4H_2NO_2$		✓ (m)	✓ (m)	✓ (s)
95.024	$C_4H_3N_2O$		✓ (w)	✓ (w)	✓ (m)
83.037	$C_4H_5NO$		✓ (vw)	✓ (vw)	✓ (w)
82.041	$C_4H_6N_2$		✓ (vw)	✓ (vw)	✓ (w)
81.045	$C_4H_5N_2$		✓ (vw)	✓ (vw)	✓ (s)
68.013	$C_3H_4N_2$		✓ (vw)	✓ (vw)	✓ (vw)
67.029	$C_3H_3N_2$		✓ (vw)	✓ (vw)	✓ (vw)

55.030	C <sub>3</sub> H <sub>5</sub> N		✓ (vw)	✓ (vw)	✓ (vw)
54.034	C <sub>3</sub> H <sub>4</sub> N		✓ (vw)	✓ (vw)	✓ (w)
53.002	C <sub>3</sub> HO		✓ (vw)	×	✓ (vw)

Intensity is relative to total fragment yield, the % for HCD are for the 0-24% HCD energy range which is approximately equivalent to the experiment  $h\nu$  range. The (s/m/w/vw) classification of the relative ion production rates follows the key given in the main text.

### S6: Photofragment Production Spectra for Minor Photofragments.

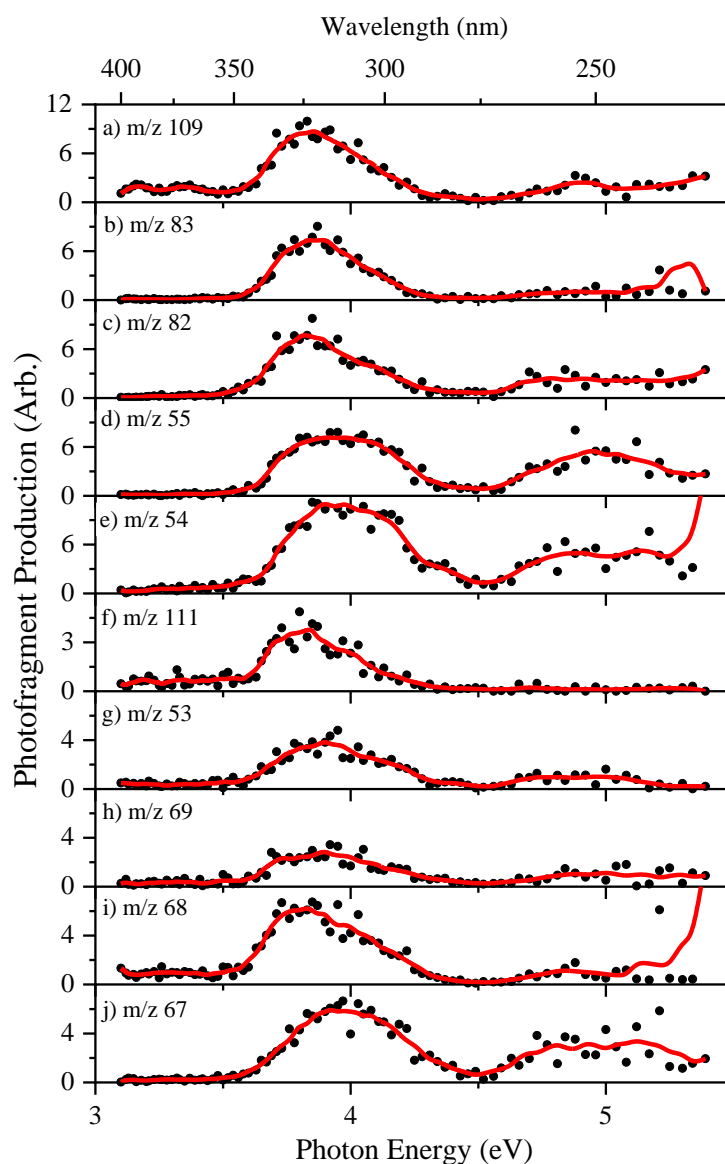


**Figure S4:** Photofragment production spectra of minor photofragments (a) m/z 109, (b) m/z 83, (c) m/z 82, (d) m/z 55, (e) m/z 54, (f) m/z 111, (g) m/z 53, (h) m/z 69, (i) m/z 68 and (j) m/z 67 produced via electrospray ionisation from a solution of water across the range 3.1-5.4 eV (400-229 nm). Solid lines are a 5-point adjacent average of data points.

### S7: High-Energy Collisional Induced Dissociation Spectra

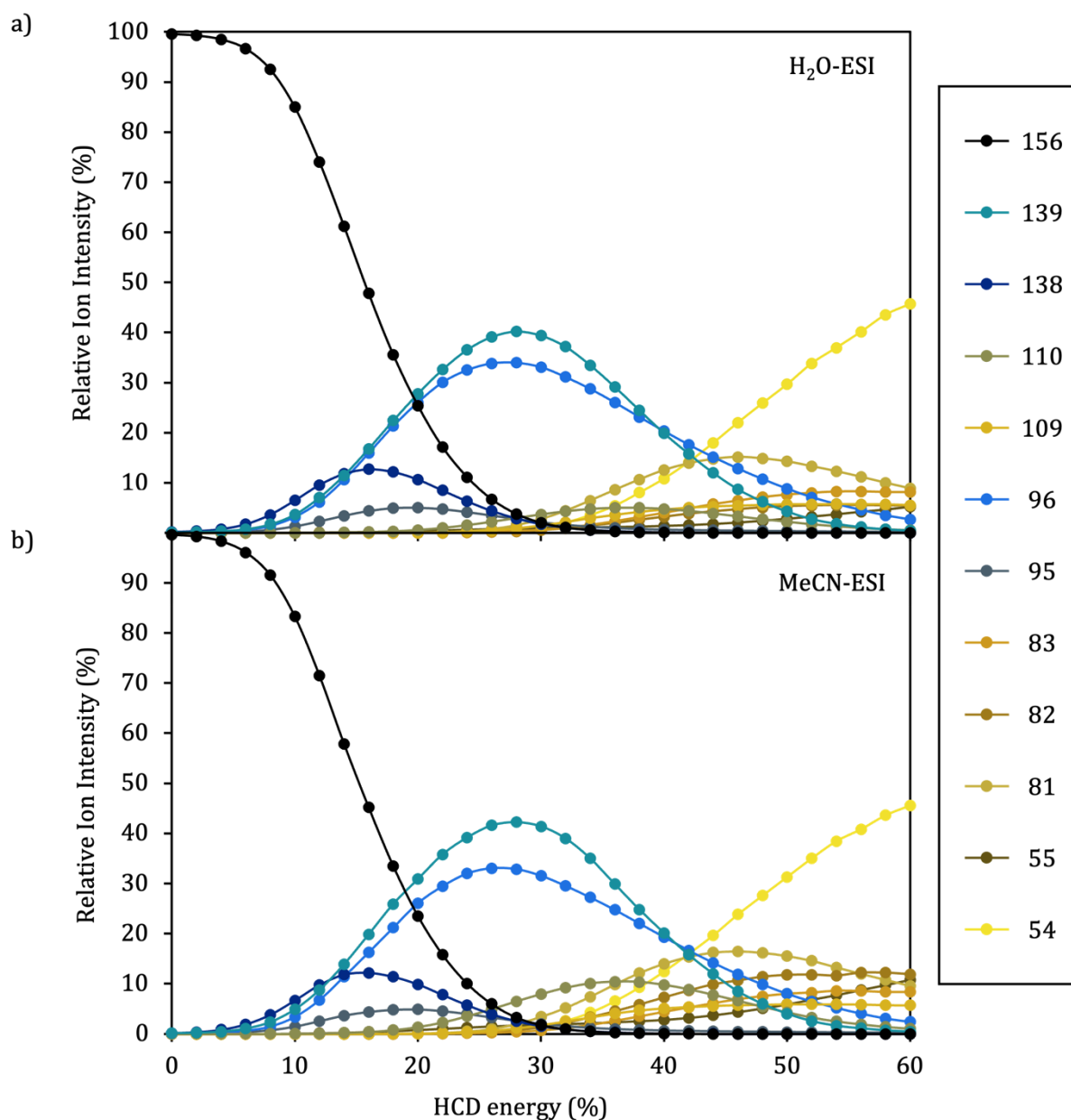


**Figure S5:** % Decay curve for mass selected  $[Z+H]^+$  ion ( $m/z$  156) and associated % fragment production curves for major thermal fragments on high-energy CID over the range 0-40 % HCD energy, in (a) H<sub>2</sub>O-ESI and (b) MeCN-ESI. Data points are an average of five repeats and solid lines are a five-point adjacent average of data points.

**S8: Histograms showing the relative ion yields of photofragments and HCD fragments.**

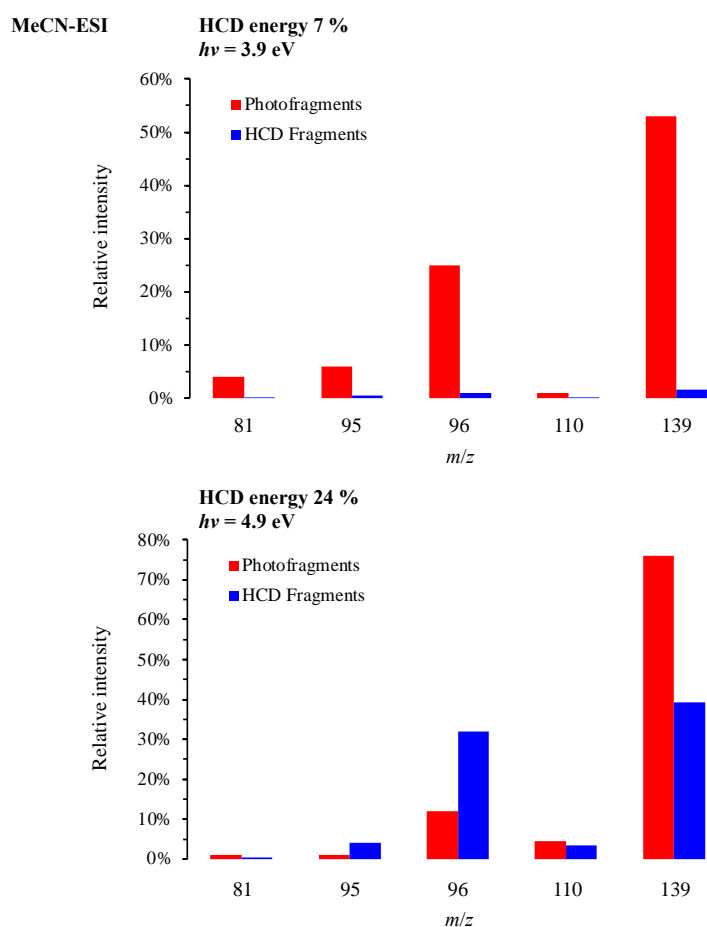


**Figure S6:** Histogram showing the relative ion yield of the highest intensity  $m/z$  fragments, produced via photoexcitation (red) and HCD (blue), in the MeCN-ESI experiments. Two separate energy regimes are shown, corresponding approximately to the maxima of band I (top) and band II (bottom).

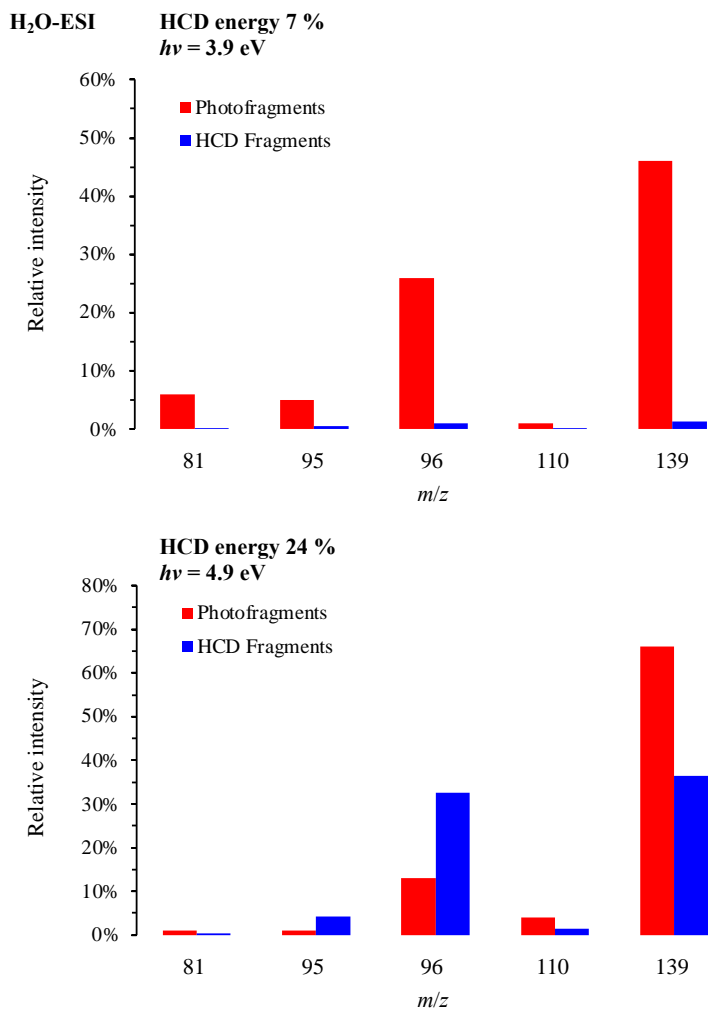


**Figure S7:** Histogram showing the relative ion yield of the highest intensity  $m/z$  fragments, produced via photoexcitation (red) and HCD (blue), in the H<sub>2</sub>O-ESI experiments. Two separate energy regimes are shown, corresponding approximately to the maxima of band I (top) and band II (bottom).

### S9: Cartesian Coordinates of the Protomers of Z

Minimum energy structures optimised at MP2/cc-pVDZ

#### N4\_enol

6	-1.376981	1.270299	0.057056
6	0.002752	1.266829	-0.108027
6	0.738593	2.433275	-0.114362
6	0.101487	3.681655	0.049064
6	-1.994480	2.491485	0.216237
1	-1.950706	0.357089	0.061732
1	0.540085	0.337541	-0.237216
7	-1.251160	3.626029	0.206778
7	0.691905	4.869736	0.061617
1	1.696881	4.879606	-0.057760
1	0.175222	5.724518	0.183128
7	2.188002	2.339341	-0.294096
8	2.825780	3.395130	-0.296454
8	2.661145	1.223496	-0.428664
8	-3.282388	2.747461	0.388010
1	-3.800791	1.930372	0.392799
1	-1.769870	4.490482	0.329208

#### N7O-enol

6	-1.237527	1.146025	-0.062897
6	0.096702	1.195528	-0.296972
6	0.752043	2.457122	-0.210116
6	-0.009008	3.639231	0.120836
6	-1.906683	2.372222	0.258569
1	-1.802680	0.228263	-0.110034
1	0.661551	0.310743	-0.543815
7	-1.330260	3.551513	0.346322
7	0.532689	4.840459	0.218470
1	1.518795	4.982227	0.062626

1	-0.078646	5.608984	0.454785
7	2.085446	2.562062	-0.434998
8	2.771070	3.575567	-0.394106
8	2.705699	1.384688	-0.739623
8	-3.198341	2.279157	0.477811
1	-3.542752	3.164935	0.684809
1	3.635287	1.659602	-0.863490

### **N7O-keto**

6	1.512732	-1.482372	-0.000003
6	0.162819	-1.477845	-0.000002
6	-0.563724	-0.240923	-0.000001
6	0.137510	1.018064	-0.000001
6	2.276454	-0.244258	-0.000002
1	2.078792	-2.401324	-0.000005
1	-0.392876	-2.402317	-0.000003
1	2.022608	1.800366	-0.000002
7	1.471332	0.947662	-0.000002
8	3.476174	-0.123234	-0.000005
7	-0.476627	2.186242	-0.000000
1	-1.488934	2.199373	0.000000
1	0.044085	3.050207	-0.000000
7	-1.915297	-0.226093	0.000000
8	-2.665475	0.747035	0.000001
8	-2.488731	-1.465672	-0.000000
1	-3.442953	-1.255088	0.000001